Dual Focal Splines and Rational Curves with Rational Offsets

by

Marian Neamtu [1], Helmut Pottmann [2], and Larry L. Schumaker [3]

Abstract. We review the theory of homogeneous splines and their relationship to special rational splines considered by J. Sánchez–Reyes and independently by P. de Casteljau who called them focal splines. Applying an appropriate duality, we transform focal splines into a remarkable class of rational curves with rational offsets. We investigate geometric properties of these dual focal splines, and discuss applications to curve design problems.

1. Introduction

In this paper we discuss an interesting connection between trigonometric splines and a class of rational splines introduced by J. Sánchez–Reyes [29,30] and independently by P. de Casteljau [2], who called them *focal splines*. The properties of homogeneous and trigonometric splines (see Sects. 2 and 3) suggest the study of a class of rational spline curves which generalize the classical NURBS curves. In Sect. 4 we show that focal splines are contained in this class of rational splines, and that they can be viewed as graphs of trigonometric splines. Moreover, a special polarity map transforms focal splines into dual focal splines consisting of a remarkable class of rational curves whose offset curves are also rational (Sect. 5). We finish the

[1] Department of Mathematics, Vanderbilt University, Nashville, TN 37240, neamtu@math.vanderbilt.edu. Partially supported by Vanderbilt University Research Council.

[2] Institute of Geometry, Technical University of Vienna, Wiedner Hauptstraße 8–10, A-1040 Vienna, pottmann@geometrie.tuwien.ac.at. Supported by the Austrian Science Foundation through project P09790.

[3] Department of Mathematics, Vanderbilt University, Nashville, TN 37240, s@mars.cas.vanderbilt.edu. Supported by the National Science Foundation under grant DMS-9500643 and by NATO under grant CRG-951291.

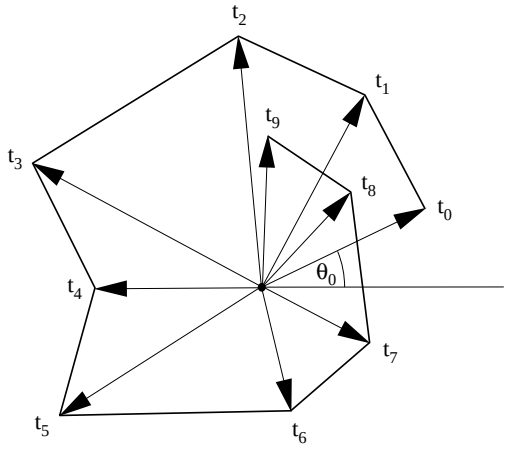

Fig. 1. A knot polygon.

paper with some examples and a discussion of potential applications. A detailed description of the use of dual focal splines in the design of cam profiles is given in [22].

2. Homogeneous Splines

In this section we briefly review the theory of homogeneous splines, cf. [12,13,35]. Let $T := \{t_i\}_{i=0}^{k+n+1}$ be a knot sequence consisting of nonzero vectors in $\mathbb{R}^2$. Each knot t_i is characterized by its polar angle θ_i and its polar radius $\rho_i > 0$. We assume that the sequence $\{\theta_i\}_{i=0}^{k+n+1}$ is nondecreasing with $0 < \theta_{i+k+1} - \theta_i < \pi$, and that $t_i = t_j$ whenever $\theta_i = \theta_j$. The polygon connecting the vertices t_i will be called the *knot polygon*. It may wind around the origin more than once, but in such a way that any $k+2$ consecutive vertices define a turning angle less than π, see Fig. 1.

Given two linearly independent vectors v_1, v_2, every $v \in \mathbb{R}^2$ is uniquely represented as $v = b_1 v_1 + b_2 v_2$ with

$$b_1 = \frac{d(v, v_2)}{d(v_1, v_2)}, \quad b_2 = \frac{d(v_1, v)}{d(v_1, v_2)},$$

where $d(v_1, v_2)$ is the determinant of the matrix whose columns are the vectors v_1 and v_2. The numbers b_1, b_2 are the coordinates of v with respect to v_1, v_2, which reduce to the usual coordinates if $t_i = (1, y_i)$ and $t = (1, y)$. It will be convenient to introduce the *wedges* $[v_1, v_2] := \{b_1 v_1 + b_2 v_2, b_1, b_2 \geq 0\}$, $[v_1, v_2) := \{b_1 v_1 + b_2 v_2, b_1 \geq 0, b_2 > 0\}$, etc., as counterparts of real intervals.

The *normalized homogeneous B-splines* $\{N_i^k\}_{i=0}^n$ of degree k are defined by the recurrence

$$N_i^r(v) := \frac{d(v, t_i)}{d(t_{i+r}, t_i)} N_i^{r-1}(v) + \frac{d(t_{i+r+1}, v)}{d(t_{i+r+1}, t_{i+1})} N_{i+1}^{r-1}(v), \quad r = 1, \ldots, k, \qquad (2.1)$$

where the lowest-degree B-splines are given by

$$N_i^0(v) := \begin{cases} 1, & \text{for } v \in [t_i, t_{i+1}) \\ 0, & \text{otherwise.} \end{cases}$$

For a knot polygon that winds around the origin more than one complete rotation, some vectors v belong to more than one wedge $[t_i, t_{i+1})$. Thus in using recurrence (2.1), it is necessary to know which wedge to consider. A way to formalize this is to express vectors in terms of polar coordinates with polar angles varying from a starting value, say 0, to the total rotational angle of the knot polygon.

The functions N_i^k are *piecewise homogeneous polynomials* of degree k supported on $[t_i, t_{i+k+1}]$. They are analogs of the classical polynomial B-splines. Also known as truncated power functions or cone splines, these functions were introduced by Dahmen [3] (see also [21]).

A *homogeneous spline curve* s with control points $D_0, \ldots, D_n$ in $\mathbb{R}^d$ is defined by

$$s(v) = \sum_{i=0}^{n} D_i N_i^k(v). \tag{2.2}$$

One may also consider homogeneous spline curves to be defined in the projectively extended Euclidean d-space $\mathbb{P}^d$ by considering the control points D_i as points in $\mathbb{P}^d$. It is customary to express a point X in $\mathbb{P}^d$ in terms of homogeneous Cartesian coordinates $X = (X_0, \ldots, X_d)$ with the convention that points at infinity are characterized by $X_0 = 0$. For each $i = 0, \ldots, n$, we suppose that the homogeneous representation of the control point D_i is the vector $D_i = (D_i^0, \ldots, D_i^d)$.

Note that (2.2) indeed represents a curve in $\mathbb{P}^d$, since by homogeneity of the basis functions, the set $\{s(\lambda v), \lambda > 0\}$ represents a single point in $\mathbb{P}^d$. This means that it suffices to evaluate $s(v)$ for v on the knot polygon. To draw the curve, we sample the polygon and thereby always know which sheet of the domain we are on.

If the *weights* D_i^0 are positive, the control points can be connected by affine line segments, and we obtain the usual *affine control polygon*. Instead of weights, we can use *frame points* as geometric input. These are the points with homogeneous coordinate vectors $F_i := D_i + D_{i+1}$, $i = 0, \ldots, n-1$. The frame points may be used to define a *projective control polygon* which consists of those segments of the projective lines $D_i D_{i+1}$ containing F_i, see [20,23]. For positive weights, the projective control polygon coincides with the affine control polygon.

From the homogeneous piecewise polynomial representation, it is clear that the curves (2.2) are *piecewise rational*. Introducing the cumulative arc length of the knot polygon as a parameter, we see that the curve representation is generally only C^0. However, with respect to the polar angle of the parameter domain, the curve is $C^{k-\mu}$ at a knot with multiplicity μ. Therefore, in standard CAGD terminology [4], homogeneous spline curves are (special) *rational geometric splines*. When the knot polygon lies on a line, we get the familiar NURBS curves.

It is known [34,35] that if $t_j < t_{j+1}$ and $j \le i \le j+k$, then the coefficient D_i is given by

$$D_i = S_j(t_{i+1}, \ldots, t_{i+k}), \tag{2.3}$$

where $S_j(v_1, \ldots, v_k)$ is the (homogeneous) *polar form* of s restricted to $[t_j, t_{j+1})$, *i.e.*, S_j is the unique symmetric multi-linear function such that $S_j(v, \ldots, v) = s(v)$ for all $v \in [t_j, t_{j+1})$. This immediately implies the following *de Boor algorithm*: Given $v \in [t_j, t_{j+1})$, let

$$D_i^{[r]} := \frac{d(t_{i+k+1-r}, v)}{d(t_{i+k+1-r}, t_i)} D_{i-1}^{[r-1]} + \frac{d(v, t_i)}{d(t_{i+k+1-r}, t_i)} D_i^{[r-1]}, \quad j-k+r \le i \le j, \tag{2.4}$$

where $D_i^{[0]} := D_i,\ i = j-k, \ldots, j$. Then $s(v) = D_j^{[k]}$.

Another consequence is an algorithm for inserting a knot $t \in [t_j, t_{j+1})$ into the spline s. The new coefficients $C_0, \ldots, C_{n+1}$ of s with respect to the refined knot sequence $T \cup \{t\}$ are given by

$$C_i = \begin{cases} D_i, & 0 \le i \le j-k \\ \frac{d(t,t_i)}{d(t_{i+k},t_i)} D_i + \frac{d(t_{i+k},t)}{d(t_{i+k},t_i)} D_{i-1}, & j-k < i \le j \\ D_{i-1}, & j < i \le n+1. \end{cases} \tag{2.5}$$

For positive weights, the factors in (2.5) are nonnegative, and therefore knot insertion is a *corner cutting algorithm*. Hence, the curve (2.2) satisfies the *variation diminishing property* with respect to the control polygon. This is true for general weights in a projective sense as described in [20].

In curve design with open curves we usually use a knot vector with $(k+1)$-fold knots at the endpoints of a given interval $[a, b]$. An important special case is

$$T^* = \{a := t_0 = \cdots = t_k, t_{k+1} = \cdots = t_{2k+1} =: b\}. \tag{2.6}$$

In this case the homogeneous spline consists of only one segment, and the basis functions N_i^k are the *homogeneous Bernstein polynomials* of degree k defined by

$$B_i^k(v) := \binom{k}{i} b_1(v)^{k-i} b_2(v)^i, \quad i = 0, \ldots, k,$$

with $b_1(v) = d(v, b)/d(a, b)$ and $b_2(v) = d(a, v)/d(a, b)$. The restriction of these functions to the unit circle gives *circular Bernstein polynomials* [1] associated with the interval $[\alpha, \beta]$, where α and β are the polar angles of a and b.

3. Trigonometric Splines

Suppose all knots in T lie on the unit circle C with center at the origin O, i.e. $t_i = (\cos\theta_i, \sin\theta_i),\ i = 0, \ldots, k+n+1$. Then the restriction to C of the homogeneous spline

$$s(v) = \sum_{i=0}^{n} d_i N_i^k(v), \quad d_i \in \mathbb{R}.$$

is called a *trigonometric spline*, and is given by

$$s(\theta) = s(v(\theta)) = \sum_{i=0}^{n} d_i T_i^k(\theta), \quad v(\theta) = (\cos\theta, \sin\theta), \tag{3.1}$$

where T_i^k are the *normalized trigonometric B-splines* with knots $\theta_i, \ldots, \theta_{i+k+1}$, see [15,17,33]. Piecewise, s belongs to the space

$$\mathcal{T}_k := \begin{cases} \text{span}\{1, \cos(2\theta), \sin(2\theta), \ldots, \cos(k\theta), \sin(k\theta)\}, & k \text{ even}, \\ \text{span}\{\cos(\theta), \sin(\theta), \cos(3\theta), \sin(3\theta), \ldots, \cos(k\theta), \sin(k\theta)\}, & k \text{ odd}. \end{cases}$$

of trigonometric polynomials of degree k. The coordinates b_1 and b_2 of a vector $v = (\cos\theta, \sin\theta)$ with respect to two knots $t_i, t_k \in C$ are (see [1])

$$b_1 = \frac{\sin(\theta_k - \theta)}{\sin(\theta_k - \theta_i)}, \quad b_2 = \frac{\sin(\theta - \theta_i)}{\sin(\theta_k - \theta_i)}, \tag{3.2}$$

and hence (2.1) coincides with the familiar three-term recurrence for trigonometric B-splines, see [12,15,17,33].

The similarity between polynomial and trigonometric splines is not unexpected since the normal curves of $\mathcal{T}_k$ in the sense of [23] are rational curves of degree k, and so are the normal curves of polynomials of degree k. Hence, the polar forms of trigonometric spline segments agree up to a reparameterization with the multi-projective polar forms of rational curves. We recall that the polar form of a trigonometric polynomial [10,11] can be obtained by homogeneously extending it to a bivariate homogeneous polynomial and by restricting the polar form of this polynomial to C.

4. Focal Spline Curves

In this section we discuss another special class of homogeneous splines. These curves have been investigated by J. Sánchez–Reyes [30] (without reference to the literature on trigonometric and homogeneous splines), and can be viewed as graphs of trigonometric spline functions. The same curves have also been studied independently by P. de Casteljau [2], who called them *focal splines*. Given a spline $s(\theta)$ as in (3.1), consider

$$g(\theta) = (s(\theta), \cos k\theta, \sin k\theta). \tag{4.1}$$

It is known (cf. [15,19]) that

$$\cos k\theta = \sum_{i=0}^{n} \cos(k\xi_i) T_i^k(\theta)$$

$$\sin k\theta = \sum_{i=0}^{n} \sin(k\xi_i) T_i^k(\theta),$$

where

$$\xi_i := \frac{1}{k} \sum_{j=i+1}^{i+k} \theta_j. \tag{4.2}$$

Thus g is a homogenous spline, and

$$g(\theta) = \sum_{i=0}^{n} D_i T_i^k(\theta),$$

where the homogeneous coordinates of the control points D_i are

$$D_i = (d_i, \cos k\xi_i, \sin k\xi_i).$$

Instead of the weights d_i, we could use the frame points $F_i = D_i + D_{i+1}$. The point F_i lies on the line $D_i D_{i+1}$, and its polar angle is $k(\xi_i + \xi_{i+1})/2$. Thus F_i lies on the bisector of the polar rays of D_i and D_{i+1} *i.e.*, the bisector of the oriented lines passing through O with polar angles $k\xi_i$ and $k\xi_{i+1}$, respectively. Note that for a positive d_i, the orientation of the polar ray of D_i is given by the vector $\overrightarrow{OD_i}$.

The inhomogeneous representation of (4.1) is

$$(\frac{1}{s(\theta)} \cos k\theta, \frac{1}{s(\theta)} \sin k\theta). \tag{4.3}$$

The curve g is a *graph* of the function s obtained by plotting the points whose polar coordinates are $(1/s(\theta), k\theta)$, see Fig. 2.

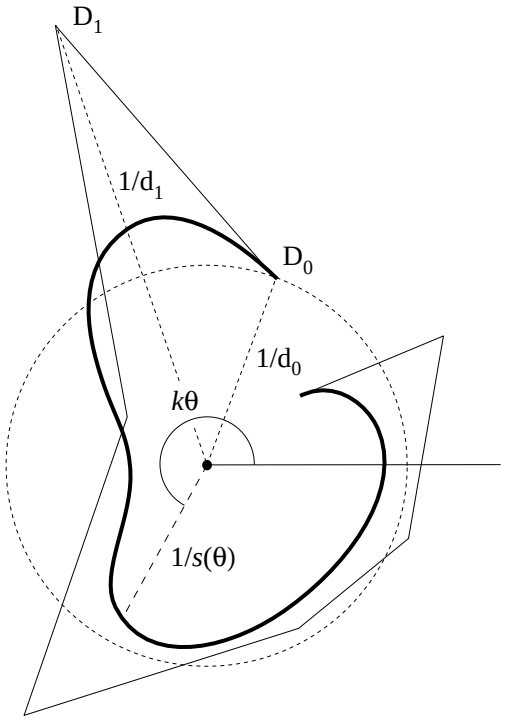

Fig. 2. Graph of a trigonometric spline s in the sense of (4.3).

The control points D_i are consistent with the graph (4.3) since they are obtained by plotting the reciprocal values of the spline coefficients $1/d_i$ on the polar ray with polar angle $k\xi_i$. For $d_i = 0$, D_i is a point at infinity. Summarizing, we have

Theorem 4.1. *Let s be a trigonometric spline given by (3.1) and let g be its associated focal spline curve whose graph (4.3) has polar coordinates $(r, \phi) := (1/s(\theta), k\theta)$. Then g is a homogeneous spline of degree k whose control points D_i have polar coordinates*

$$(r_i, \phi_i) := (\frac{1}{d_i}, k\xi_i), \quad i = 0, \ldots, n.$$

The weights of g are equal to the coefficients d_i, and its frame points F_i lie on the bisectors of the polar rays of D_i and D_{i+1}. Moreover, if S is the polar form of one of the trigonometric pieces of s, then the polar form G of the focal spline curve g corresponding to the same piece of s is given by

$$G(\theta_1, \ldots, \theta_k) = (S(\theta_1, \ldots, \theta_k), \cos(\theta_1 + \cdots + \theta_k), \sin(\theta_1 + \cdots + \theta_k)). \qquad (4.4)$$

The polar distance of the point $G(\theta_1, \ldots, \theta_k)$ is $1/S(\theta_1, \ldots, \theta_k)$, while its polar angle is $\theta_1 + \cdots + \theta_k$.

If we choose the special knot sequence (2.6) with no interior knots, then the corresponding focal spline curve g consists of a single rational Bézier curve, called a *focal Bézier curve*. In the sense of the previous section, a focal Bézier curve is the graph of a circular Bernstein-Bézier polynomial s with coefficients d_i. In order to find points on g, we can apply the classical de Casteljau algorithm (see Fig. 3). Alternatively, one can use the circular arc corresponding to $[\alpha, \beta]$ as a parameter domain, and use (2.4) to compute $s(\theta)$, based on an array of auxiliary values $d_i^{[r]}$. It follows from Theorem 4.1 that the two approaches are equivalent. In particular, we have

Theorem 4.2. [29] *Let g be a focal Bézier curve corresponding to a circular Bernstein-Bézier curve s of degree k with coefficients d_i, $i = 0, \ldots, k$, defined on a circular arc $[\alpha, \beta]$. Then, in the r-th step of the de Casteljau algorithm applied to g and $\theta \in [\alpha, \beta]$, the polar coordinates of the points $D_i^{[r]}$ are $(1/d_i^{[r]}, (k - i - r)\theta_0 + i\theta_{k+1} + r\theta)$.*

Focal Bézier curves of degree two are clearly *conics*. The angle properties illustrated in Fig. 3 imply that the origin O is a *focal point* of the conics, since the projectivity between two fixed tangents (say the end tangents) induced by the set of tangents is projected from O by a rotation. The conic tangents passing through O are the fixed lines in this rotation, hence isotropic lines (the two pencils of isotropic lines of a Euclidean plane have in each Cartesian system the complex direction

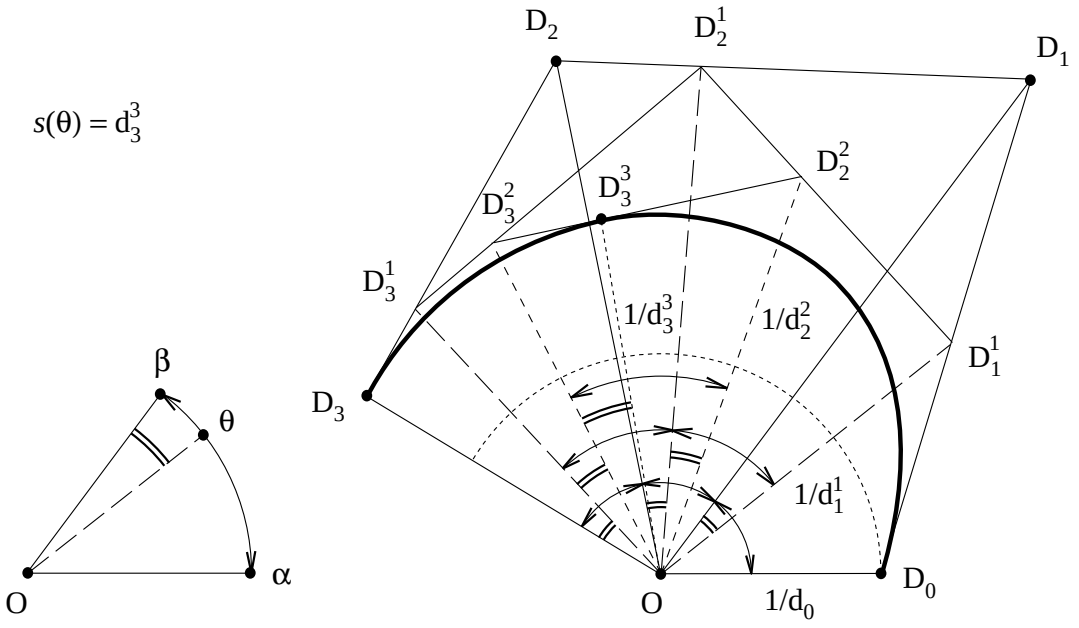

Fig. 3. de Casteljau algorithm for a focal Bézier curve.

vectors $(1, i)$ and $(1, -i)$). According to J. Plücker, this characterizes O as a focal point. A direct analytic proof follows from the polar coordinate representation and is given in [29]. This fact motivated P. de Casteljau [2] to coin the name *focal splines*. We show later (end of Sect. 5) that for arbitrary degree k, O is always a focal point of g in the sense of Plücker, i.e. the intersection of isotropic curve tangents.

Using polar coordinates (r, ϕ), consider the mapping

$$\delta : (r, \phi) \mapsto (\frac{1}{r}, \frac{\phi}{k}),$$

which is the composition of an *inversion* with a so-called *fan transformation* which multiplies each polar angle with the constant value $1/k$. Applying δ to $g(\theta)$, we obtain exactly the graph curves $p(\theta) = (s(\theta)\cos\theta, s(\theta)\sin\theta)$ discussed in [1]. The projective control polygon of g is mapped onto the curved control structure of p described in [1] for the Bézier case. Thus, algorithms for focal Bézier curves correspond to the algorithms for CBB curves given in [1]. Moreover, the control curves for trigonometric splines introduced in [15] for graphs of the form $(\theta, s(\theta))$ are related to the control polygons for focal spline curves by a transcendental transformation.

5. Dual Focal Splines

In this section we investigate a remarkable class of *rational curves with rational offsets* (also called *rational PH curves* [24,25]). We need a description of curves

which is closely related to the polar coordinate representation. Assuming that the curve c to be described is C^1, piecewise C^2 and free of inflection points, we impose an orientation on its tangents and represent them in the form

$$T(\phi): \; x\cos(\phi) + y\sin(\phi) = h(\phi), \; \phi \in [a, b].$$

Thus, ϕ is the angle between the x-axis and the normal, and h is the signed distance of the tangent to the origin, see Fig. 4. The function $h(\phi)$ is called the *support function of* c.

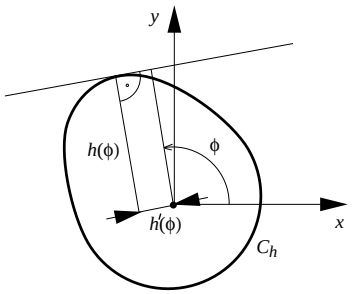

Fig. 4. A curve defined by a support function.

The curve c is the envelope of the lines $L(\phi)$, and (cf. [36]) admits the parametric representation $c = \{(x(\phi), y(\phi)), \phi \in [a, b]\}$ with

$$\begin{aligned} x(\phi) &= h(\phi)\cos(\phi) - h'(\phi)\sin(\phi), \\ y(\phi) &= h(\phi)\sin(\phi) + h'(\phi)\cos(\phi). \end{aligned}$$

This representation also reflects the fact that the curve normals possess distance $h'(\phi)$ from the origin, see Fig. 4.

The *signed radius of curvature* of the curve c is given by

$$\rho(\phi) := h(\phi) + h''(\phi). \tag{5.1}$$

A closed curve c is *convex* if and only if $\rho(\phi)$ has no sign change in $[0, 2\pi]$. The *length of the curve* c is given by

$$L = \int_a^b [h(\phi) + h''(\phi)]d\phi.$$

Using support functions one can easily express offset curves. Namely, c_d with support function $h_d(\phi) := d + h(\phi)$ is the *offset curve at signed distance* d *from* C_h. For more details on the description of curves with help of their support function, see [36].

A focal spline curve g of degree k is characterized by a polar equation $r(\phi) = 1/s(\phi/k)$, where s is a trigonometric spline function of degree k and the origin O

is the focal point of g. We now apply the *polarity* Π with respect to the unit circle C with center O. It maps each point $(\bar{x}, \bar{y})$ onto the line $\bar{x}x + \bar{y}y = 1$. Hence the points of g are mapped to the lines $x\cos(\phi) + y\sin(\phi) = s(\phi/k)$. The envelope of this family of lines is defined as image curve $p := \Pi(g)$ and will be called a *dual focal spline curve*. We see that the support function of p is

$$h(\phi) = s(\phi/k). \tag{5.2}$$

To explore the properties of p, we need to work with polarities. First, we extend the definition of Π to the entire projective plane and use homogeneous Cartesian coordinates (x_0, x_1, x_2) for points. Lines are solutions of linear homogeneous equations $u_0x_0 + u_1x_1 + u_2x_2 = 0$ and (u_0, u_1, u_2) are the homogeneous line coordinates. A point $X = (x_0, x_1, x_2)$ is then mapped under Π onto the line $L = \Pi(X) = (-x_0, x_1, x_2)$. All points of L are mapped to lines passing through X. Therefore, we extend the map Π by its dual (for simplicity also denoted by Π), which maps L onto X. We thus have a map which transforms points to lines and lines to points. The points of the circle C are mapped to its tangents and vice versa. Points and tangents of a curve are mapped to tangents and points of the image curve. A rational curve of algebraic order k and algebraic class ℓ (= algebraically counted number of tangents passing through a point) is mapped to a rational curve of order ℓ and class k. Furthermore, Π preserves contact of order r between two curves.

Since focal spline curves g are rational splines of order k with geometric continuity $C^{k-\mu}$ at a knot of multiplicity μ, we immediately have

Theorem 5.1. *Let g be a focal spline curve of degree k with focal point O. Then, a polarity with respect to a circle centered at O transforms g into a dual focal spline curve p. This is a rational geometric spline curve with geometric continuity $C^{k-\mu}$ at a knot of multiplicity μ.*

A standard NURBS representation of a spline curve requires a knot vector where all inner knots appear with multiplicity k. This implies that the control points of this curve agree with the Bézier points of the spline segments. We will therefore now restrict our attention to the segments of dual focal splines *i.e.,* to *dual focal Bézier curves*. Let g be a focal Bézier curve with control points $D_i = (d_i, \cos\phi_i, \sin\phi_i)$ corresponding to $\alpha_i = (k-i)\alpha + i\beta$. The points of the curve have homogeneous coordinates $\sum D_i B_i^k(\phi)$ and therefore the tangents of its image curve p under Π have the line coordinates

$$T(\phi) = \sum_{i=0}^{k} L_i B_i^k(\phi), \quad \text{with } L_i = (-d_i, \cos\phi_i, \sin\phi_i). \tag{5.3}$$

This is the so-called *dual representation* of the Bézier curve p introduced into CAGD by Hoschek [14], see also [26]. The lines $L_i = \Pi(D_i)$ are the *Bézier lines* of the

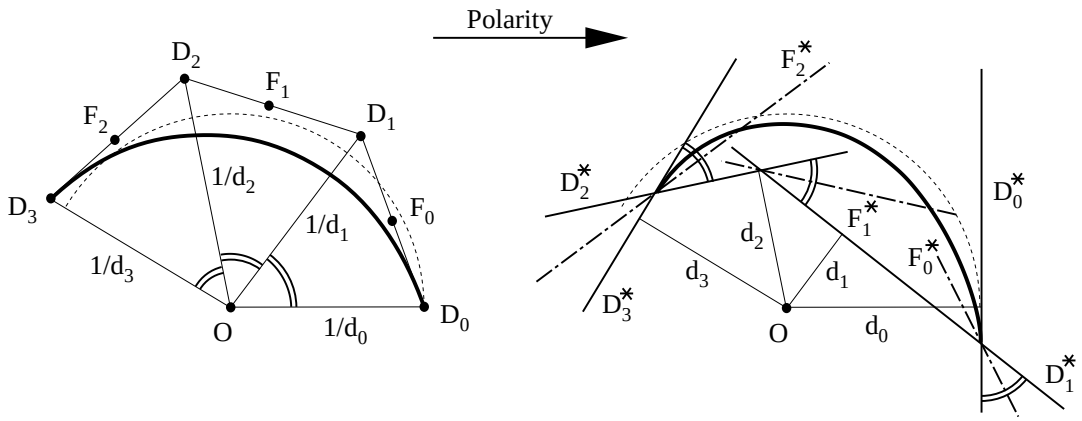

Fig. 5. Polarity applied to a focal cubic Bézier curve.

curve. We see that consecutive oriented Bézier lines L_i, L_{i+1} of p all form an angle of size $\beta - \alpha$, and the frame lines $F_i^* := L_i + L_{i+1}$ are simply the bisectors of L_i, L_{i+1}, see Fig. 5.

The *computation* of p follows directly from (5.3). We apply the algorithm of de Casteljau to the vectors $L_0, \ldots, L_k$, until there are just two vectors $L_0^{k-1}(\phi)$ and $L_1^{k-1}(\phi)$ left. These vectors represent lines through the desired curve point $p(\phi)$ which is therefore computable as the vector product $p(\phi) = L_0^{k-1}(\phi) \times L_1^{k-1}(\phi)$. This immediately leads to the following parametric representation of p as a rational Bézier curve of degree $2k-2$:

$$p(\phi) = \sum_{i=0}^{2k-2} P_i B_i^{2k-2}(\phi),$$

where

$$P_l = \frac{1}{\binom{2k-2}{l}} \sum_{i+j=l} \binom{k-1}{i} \binom{k-1}{j} L_i \times L_{j+1}. \tag{5.4}$$

One can show that $p(\phi) \neq 0$ for all ϕ, and therefore a degree reduction is not possible. Thus, the algebraic order of p is exactly $2k-2$ and we have proved the following result.

Theorem 5.2. *Let g be a focal spline curve of degree k with focal point O, and let p be the associated dual focal spline. Then, each segment of p is a rational curve of algebraic order $2k-2$ and class k. In the dual Bézier representation of p, consecutive oriented Bézier lines L_i, L_{i+1} form the same angle and the frame lines F_i^* are their bisectors.*

The support function (5.2) shows that dual focal Bézier curves are so-called *higher cycloidal trochoids* [39]. They arise as envelopes of straight lines under special planar one–parameter motions (trochoidal motions) which are composed of

a finite number of continuous rotations ρ_i with constant angular velocities ω_i. In our case, the ratio of the angular velocities of any two of these generating rotations is rational, and therefore the curves and their offsets are *rational* [39]. This can also be seen by computing the parametric representation from the support function, which yields a curve representation with sine and cosine terms of rational multiples of ϕ and thus the representation can be rationalized by standard substitutions. For k even, the space of trigonometric splines contains constants, and in this case the offset curves at distance d with support function $h(\phi)+d$ are also of the same kind.

Theorem 5.3. *Dual focal spline curves possess piecewise rational offset curves. In particular, all offsets of a dual focal spline p with even class k are dual focal splines of the same kind.*

Theorem 5.4. *Consider a dual Bézier curve p with Bézier lines L_i and frame lines F_i^* such that all consecutive oriented Bézier lines L_i, L_{i+1} form a constant angle and the frame lines F_i^* are their bisectors. Then all offsets of p are rational.*

We conclude this section by justifying the name "focal spline". Since dual focal spline segments are cycloidal trochoids, it is known that they pass through the absolute points [39], i.e., the complex points with homogeneous Cartesian coordinates $(0,1,i)$ and $(0,1,-i)$. The polarity $\Pi^{-1}=\Pi$ maps these points to lines with coordinates $(0,1,\pm i)$. They are the isotropic lines through O and tangents of g, such that O appears as focal point. Thus the origin O of the polar coordinate system which we used to define a focal spline curve as a graph of a trigonometric spline is a focal point for each spline segment g in the sense of J. Plücker. This means that it is the intersection of isotropic curve tangents of the algebraic curve g in the complex projective plane.

6. Conversion of Dual Focal Splines to NURBS

To convert from the support function (5.2) to the rational representation, we can perform knot insertion on the trigonometric spline s until each inner knot appears with multiplicity k. Denote the new trigonometric spline coefficients by b_i. The spline segment over the interval $[\theta_{j-1},\theta_j]$ leads to a focal Bézier curve segment p_j of p, whose normals have directional angles in $[k\theta_{j-1},k\theta_j]$. The curve p_j has a dual Bézier representation, whose control lines $L_0,\ldots,L_k$ possess the homogeneous line coordinates $L_i=(-b_{(j-1)k+i+1},\cos(\phi_i),\sin(\phi_i))$ with $\phi_i:=(k-i)\theta_{j-1}+i\theta_j$. With L_i we compute the homogeneous coordinates P_l of the control points of the rational Bézier curve p_j with the help of (5.4).

7. Examples

We now examine a few simple examples.

Example: $k=2$. The dual focal Bézier curve has a support function of the form

$$h(\phi)=a_0+a_1\cos\phi+a_2\sin\phi,$$

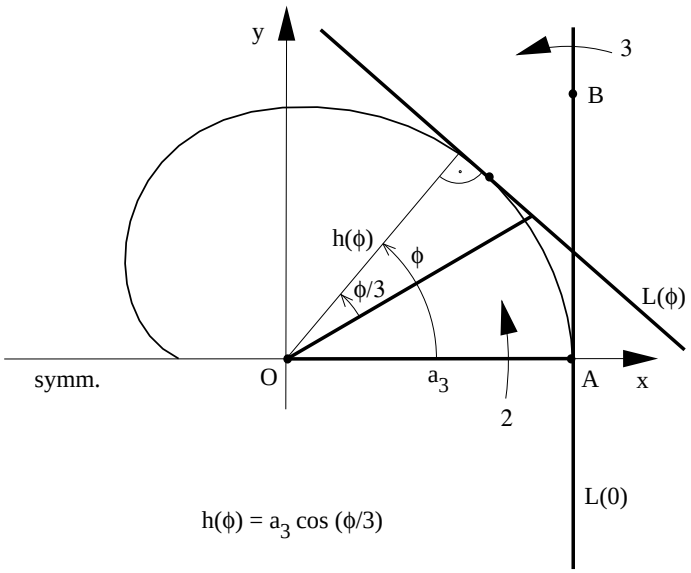

Fig. 6. A dual focal Bézier curve of degree 3.

and thus is a *circle* with radius a_0 and center (a_1, a_2). For $a_0 = 0$ it degenerates to a point. Therefore, with $k = 2$, focal splines are *arc splines*. We see that arc spline approximations of a curve c may also be obtained by splitting c at inflections, describing the noninflecting pieces by their support functions and approximating these with trigonometric splines of degree 2. A multiresolution analysis of arc splines based on this idea has recently been proposed by J. Wallner [38].

Example: $k = 3$**.** In this case the dual focal Bézier curve is a rational quartic of class 3 with the support function

$$h(\phi) = a_1 \cos\phi + a_2 \sin\phi + a_3 \cos\frac{\phi}{3} + a_4 \sin\frac{\phi}{3}.$$

The kinematic generation as a cycloidal trochoid is as follows. Consider two moving lines OA and $l = AB$, such that OA rotates around O with angular velocity 2 and l rotates around A with angular velocity 3, see Fig. 6. Then, the envelope of l is a quartic of the present kind and is called a *cardioid*.

Example: $k = 4$**.** In this case we get dual focal Bézier curves with a support function

$$h(\phi) = a_0 + a_1 \cos\phi + a_2 \sin\phi + a_3 \cos\frac{\phi}{2} + a_4 \sin\frac{\phi}{2}.$$

The curves are rational curves of order 6 and class 4. Kinematically, they are obtained as the envelope of a line under a motion composed of two rotations with angular velocities $\omega_1 : \omega_2 = 1 : 2$ (see Fig. 7). For $a_0 = 0$, the generating line passes through the second rotation center, in which case the envelope is a so-called *nephroid*. Otherwise, the curves are offsets of nephroids. The corresponding focal

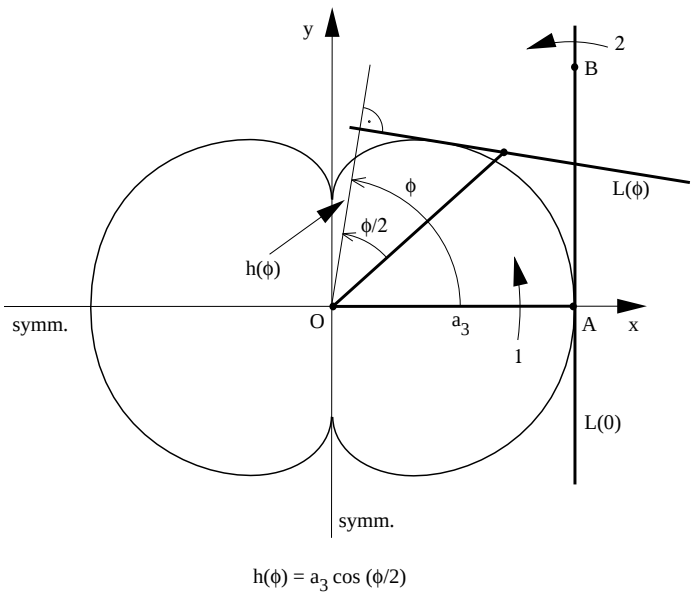

Fig. 7. A dual focal Bézier curve of degree 4.

spline curves have third order geometric continuity (at single knots), and their offsets are of the same type. This is the first example we have seen of a low order PH spline curve with third order geometric continuity.

8. Applications

The fact that the support function (5.2) of dual focal splines is basically a trigonometric spline allows us to solve certain curve design problems in a surprisingly simple way. In particular, the fact that they are piecewise rational and thus representable in standard CAD/CAM systems, makes them especially useful for the design of *cam profiles* [22], constant length curves [27,28] and other curves which arise in NC milling and layered manufacturing, see [5,6,7,24,25] and the references therein.

Rational PH curves have been an active area of CAGD research in the past few years (see e.g., [8,9]). Using our class of rational curves with rational offsets, we can guide the shape of a Bézier curve via its dual representation, see [14,25]. This means we can interactively design rational PH curves by keeping the angles between consecutive control lines constant.

References

1. Alfeld, P., M. Neamtu, and L. L. Schumaker, Circular Bernstein-Bézier polynomials, in *Mathematical Methods for Curves and Surfaces,* Morten Dæhlen, Tom Lyche, Larry L. Schumaker (eds), Vanderbilt University Press, Nashville & London, 1995, 11–20.

2. Casteljau, P. de, Splines focales, in *Curves and Surfaces in Geometric Design,* P.-J. Laurent, A. Le Méhauté, and L. L. Schumaker (eds), A. K. Peters, Wellesley MA, 1994, 91–103.
3. Dahmen, W., On multivariate B-splines, SIAM J. Numer. Anal. **17** (1980), 179–191.
4. Farin, G., *Curves and Surfaces for CAGD,* 3rd ed., Academic Press, Boston, 1993.
5. Farouki, R. T., Pythagorean hodograph curves in practical use, in *Geometry Processing for Design and Manufacturing,* R. E. Barnhill (ed), SIAM, Philadelphia, 1991, 3–33.
6. Farouki, R. T. and H. Pottmann, Polynomial and rational Pythagorean hodograph curves reconciled, IBM Research Report RC19571, 1994.
7. Farouki, R. T., K. Tarabanis, J. U. Korein, J. S. Batchelder, and S. R. Abrams, Offset curves in layered manufacturing, ASME Manufacturing Science and Engineering Book G0930B, PED-Vol. **68-2** (1994), 557–568.
8. Farouki, R. T. and S. Shah, Real-time CNC interpolators for Pythagorean hodograph curves, Comput. Aided Geom. Design **13** (1996), 583–600.
9. Farouki, R. T., S. Jee, and J. Manjunathaiah, Design of rational cam profiles with Pythagorean-hodograph curves, preprint, 1997.
10. Gonsor, D. E. and M. Neamtu, Non–polynomial polar forms, in *Curves and Surfaces in Geometric Design,* P.-J. Laurent, A. Le Méhauté, and L. L. Schumaker (eds), A. K. Peters, Wellesley MA, 1994, 193–200.
11. Gonsor, D. E. and M. Neamtu, Null spaces of differential operators, polar forms and splines, J. Approx. Theory **86** (1996), 81–107.
12. Goodman, T. N. T. and S. L. Lee, B-splines on the circle and trigonometric B-splines, in *Approximation Theory and Spline Functions,* S. P. Singh, J. H. W. Burry, and B. Watson (eds), Reidel, Dordrecht, 1984, 297–325.
13. Goodman, T. N. T. and S. L. Lee, Homogeneous polynomial splines, Proc. Roy. Soc. Edinburgh Sect. A **117** (1991), 89–102.
14. Hoschek, J., Dual Bézier curves and surfaces, in *Surfaces in Computer Aided Geometric Design,* R. E. Barnhill and W. Boehm (eds), North Holland, Amsterdam, 1983, 147–156.
15. Koch, P. E., T. Lyche, M. Neamtu, and L. L. Schumaker, Control curves and knot insertion for trigonometric splines, Advances in Comp. Math. **3** (1995), 405–424.
16. Lyche, T. and R. Winther, A stable recurrence relation for trigonometric B-splines, J. Approx. Theory **25** (1979), 266–279.
17. Lyche, T., L. Schumaker, and S. Stanley, Quasi-interpolants based on trigonometric splines, J. Approx. Theory, to appear.

18. Mazure, M.-L. and H. Pottmann, Tchebycheff curves, preprint, 1994.

19. Neamtu, M., Homogeneous simplex splines, J. Comput. Appl. Math. **73** (1996), 173–189.

20. Neamtu, M., H. Pottmann, and L. Schumaker, Designing NURBS cam profiles using trigonometric splines, preprint, 1997.

21. Pottmann, H., The geometry of Tchebycheffian splines, Comput. Aided Geom. Design **10** (1993), 181–210.

22. Pottmann, H., Rational curves and surfaces with rational offsets, Comput. Aided Geom. Design **12** (1995), 175–192.

23. Pottmann, H., Curve design with rational Pythagorean-hodograph curves, Advances in Comp. Math. **3** (1995), 147–170.

24. Pottmann, H., Studying NURBS curves and surfaces with classical geometry, in *Mathematical Methods for Curves and Surfaces,* Morten Dæhlen, Tom Lyche, Larry L. Schumaker (eds), Vanderbilt University Press, Nashville & London, 1995, 413–438.

25. Roulier, J. A. and P. Piper, Prescribing the arc length of parametric curves, Comput. Aided Geom. Design **13** (1996), 3–22.

26. Roulier, J. A. and P. Piper, Prescribing the length of rational Bézier/ curves, Comput. Aided Geom. Design **13** (1996), 23–43.

27. Sánchez–Reyes, J., Single-valued curves in polar coordinates, Computer-Aided Design **22** (1990), 19–26.

28. Sánchez–Reyes, J., Single-valued spline curves in polar coordinates, Computer-Aided Design **24** (1992), 307–315.

29. Schumaker, L. L., *Spline Functions: Basic Theory,* Interscience, New York, 1981. Reprinted by Krieger, Malabar, Florida, 1993.

30. Seidel, H. P., A new multiaffine approach to B-splines, Comput. Aided Geom. Design **6** (1989), 23–32.

31. Strøm, K., B-splines with homogenized knots, Advances in Comp. Math. **3** (1995), 291–308.

32. Strubecker, K., *Differentialgeometrie I,* Göschen, Berlin, 1964.

33. Wallner, J., A generalized multiresolution analysis for arc splines, preprint, 1997.

34. Wunderlich, W., Höhere Radlinien, Österreichisches Ingenieur–Archiv **1** (1947), 277–296.